

# A visual observation of the air flow pattern for the high speed nozzle applicable to high power laser cutting and welding<sup>☆</sup>

Chi-Shan Tseng<sup>a</sup>, Chun-Ming Chen<sup>b</sup>, Chi-Chuan Wang<sup>a,\*</sup>

<sup>a</sup> Department of Mechanical Engineering, College of Engineering, National Chiao Tung University, Hsinchu 300, Taiwan

<sup>b</sup> Laser Application Technology Center, Industrial Technology Research Institute, Tainan 734, Taiwan

## ARTICLE INFO

Available online 6 November 2013

### Keywords:

Visual observation  
Nozzle  
Cutting and welding

## ABSTRACT

In this study, the flow pattern and pressure variation of the nozzles applicable to high power laser cutting and welding were studied. A total of five nozzles are made and tested with nozzle diameter ranging from 0.8 to 4 mm. The depth of focus and the width of focus are measured based on the flow visualization. It is found that the depth of focus is increased with the rise of exit Mach number while the width of focus is increased with the nozzle diameter. The visual results indicate that the supersonic nozzle reveals a more concentrated jet flow pattern even the flow has passed through the depth of focus. On the other hand, appreciate deviation of the flow pattern is observed for the subsonic nozzle after the depth of focus. As far as more concentrated air flow pattern is concerned, a supersonic nozzle with an exit diameter less than 3.0 mm is recommended. The total pressure decreasing tremendously with the exit Mach number is encountered while moderate decline of the static and dynamic pressure for supersonic nozzles is seen. However, its corresponding dynamic pressure is still higher than that of the subsonic nozzle.

© 2013 Elsevier Ltd. All rights reserved.

## 1. Introduction

In high power laser cutting and welding processes, the shielding gas plays an essential role. In laser cutting, high pressure and high speed air flow are needed in order to blow out the melted materials to ensure high quality of the laser cutting. In laser welding, the shielding gas protects optical lens from spatters and screens the solidifying metal from the surrounding ambient. The operational speed and pressure of the shielding gas for laser welding are generally much lower than that in laser cutting. In practical operation, the air flow speed is strongly related to the nozzle design. The nozzle affects the inlet stagnation pressure, tip to workpiece standoff distance, and width and thickness of the cut kerf on the behavior of the gas jet patterns inside the kerf [1].

There are a lot of experimental and numerical investigations on the effects of the high speed gas jet in laser cutting process. The influence of stand-off distance on laser cutting using supersonic nozzles is investigated by Chen et al. [2,3], Hu et al. [4], Man et al. [5–7] through which supersonic jet inside laser cut kerf was experimentally and numerically examined. Supersonic gas dynamic characteristic is studied by Guo et al. [8] numerically. Supersonic impinging jet inside an inclined substrate was investigated by Mai and Lin [9]. The above researches [8,9] focused on the dynamic properties of supersonic gas flow and the associated influence of impinging jet on the work piece subject to laser cutting. As pointed out by Chen et al. [2], a strong normal shock prevails in front

of the work piece and this normal shock is undesirable for Mach number after this normal shock would substantially decrease to subsonic level and it creates gigantic energy loss. Those researches focused on the influence of stand-off distance to shock structure before or inside the cut kerf. Although there are many researches on supersonic gas flow in laser cutting, the depth of focus and width of focus of high Mach number jet from supersonic nozzles had not been reported clearly. In this regard, it is the objective of this study to examine the influence of associated important parameters subject to various nozzle designs.

## 2. Experimental setup

A total of 5 nozzles were made and tested in the present study. Their detailed geometry is tabulated in Table 1. In these five nozzles, nozzles #1 to #4 are designed to attain at supersonic speed. Hence the nozzles have a divergent part in order to further accelerate the air flow to supersonic speed. Nozzle #5 is designed at sonic speed because it does not have divergent part. Note that when the upstream reservoir pressure reaches 1.89 bar or higher, the mass flow rate is choked at the throat of a nozzle and the Mach number at throat is exactly 1. The desired outlet Mach number is made by area ratio of throat to outlet area. Outlet Mach number and other parameters of each nozzle are listed in Table 1. Where  $D_o$  is outlet diameter and  $D_t$  is throat diameter.  $\theta_o$  is the open angle of the divergent part of the nozzle and  $h$  is the distance between throat and outlet tip. The distance between throat part and outlet tip ( $h$ ) for nozzle #1 and #2 are 1.5 mm and for nozzle #3 and #4 are 3 mm. By exploitation of the nozzles, various outlet Mach number can be achieved. The supersonic speed is achieved by convergent–

<sup>☆</sup> Communicated by W.J. Minkowycz.

\* Corresponding author at: EE474, 1001 University Road, Hsinchu 300, Taiwan.  
E-mail address: [cawang@mail.nctu.edu.tw](mailto:cawang@mail.nctu.edu.tw) (C.-C. Wang).

### Nomenclature

$D_o$	nozzle outlet diameter
$D_t$	nozzle throat diameter
$\theta_o$	divergent degree of nozzle
$h$	distance between nozzle throat and tip
$P_{o1}$	total pressure before normal shock wave
$P_{o2}$	total pressure after normal shock wave
$M_1$	Mach number before normal shock wave
$M_2$	Mach number after normal shock wave
$\gamma$	specific ratio of air

divergent nozzle if the upstream reservoir pressure is higher than 1.89 bar which is demonstrated by Man et al. [7] who mentioned that when the gas pressure  $P_o$  is less than 1.89 kg/cm<sup>2</sup> (0.185 MPa) (absolute pressure), velocity  $V$  and flow  $Q$  increase with the increasing of inlet pressure  $P_o$ , but when  $P_o$  reaches 1.89 kg/cm<sup>2</sup> (0.185 MPa),  $V$  attains a maximum value. A further increase in  $P_o$  also increases the flow  $Q$ , but the gas velocity will remain unchanged.

The schematic of the test facility is shown in Fig. 1 which contains an air compressor capable of providing compressed air of 5–7 bar. The compressed air is then stored in a tank. A metering valve is then used to regulate the compressed air into the test nozzles. A hi-precision Pitot tube (Dwyer, model 167 series) is used to measure the outlet static and dynamic pressure of the incoming jet flow out of the nozzle. A differential pressure transducer (Yokogawa, model EJA110A, style:S1) with a full scale resolution of 0.1% and an absolute pressure transducer (Yokogawa, model FP101A-E11-L20A\*B) having a calibrated accuracy of 0.2% is used to measure the dynamic and static pressure of the Pitot tube, respectively. The Pitot tube is placed 2 mm from the nozzle tip. In addition to the measurements of dynamic and static pressure, a high speed camera (Dongmao Instrument Scientific Co., SVSi Gigaview) is used to measure the depth of focus of the airflow from the design jet. The flow visualization is made possible by a smoke generator with particle size being around 1.3  $\mu\text{m}$ . The generated smoke is first collected in a bag, and was fed to the nozzle to mix with the compressed air from the air tank. The high speed camera is then used to record the smoke flow from the nozzle. Normally 1000–2000 pictures per second were taken with pixel resolution of 720  $\times$  480. The major effort of the flow visualization is to identify the depth of focus of the jet flow.

### 3. Results and discussion

Fig. 2 depicts the flow visualization of the five nozzles. Since the depth of focus is an important parameter in laser cutting. This is because high power laser beam can only melt the material, and it would require the associated high speed gas flow to cut the material accordingly. In this sense, the depth of focus is quite imperative since it acts as the focal point of impingent air flow that provides sufficient momentum to cut the melting material. Definition of the depth of focus (DOF) is defined as the point where the air flow starts to diverge.

As illustrated in Fig. 2(a) and Table 1, the DOF is approximate 9.5 mm with a Mach number of 1.76, and the width of focus is approximately 1.91 mm. For nozzle #2, as shown in Fig. 2(b), the corresponding DOF is approximately 12.4 mm whereas the Mach number equals to 2.3 and the width of focus is approximately 2.86 mm. It appears that the jet deviates much faster after the DOF and the width of focus becomes larger. This is because the outlet nozzle diameter is also larger. Analogously in Fig. 2(c) for nozzle #3, an attained Mach number of 2.02 is achieved and the DOF is approximately 11.9 mm and the width of focus is approximately 2.39 mm. Similar to Fig. 2(a), the jet flow does not show an appreciable deviation after DOF. This is attributed to its smaller outlet diameter of 2.55 mm. On the other hand, the largest

outlet diameter is 4.96 mm in nozzle #4. The DOF is considerably increased to 17.2 mm with the highest exit Mach number of 3.1, but a detectable deviation of the jet flow after DOF emerges. Conversely, nozzle #5 is designated with the smallest exit diameter of 0.82 mm. The DOF is reduced to 7.2 mm as expected but the air flow pattern deviates and diverges pronouncedly after the DOF as shown in Fig. 2(e). The results imply that the subsonic operation may not be appropriate for the flow pattern scatters notably after DOF. The visual results for the more concentrated jet flow stream under supersonic operation can be substantiated by the diamond structure as shown in Fig. 3 formed by an under-expanded jet impinging on to a flat plate [3,8]. The air flow is confined within the boundary and reveals a less scattering. In the meantime, to avoid a larger deviation of flow pattern after DOF for supersonic operation, an exit diameter less than 3.0 mm is more appropriate based on the present visualization. The results are in line with all the previous investigations since the nozzle diameters for all the studies falls between 0.8 and 1.7 mm (e.g. Man et al. [1,5–7];  $D_o = 0.8\text{--}1.5, 1.6, 1.7$  mm; Chen et al. [3],  $D_o = 1.35$  mm; Hu et al. [4],  $D_o = 1.6$  mm; Mai and Lin [9],  $D_o = 1.5$  mm).

Summarization from the foregoing discussion, it is found that the DOF is strongly related to the exit Mach number. This is applicable for both supersonic nozzles (#1–#4) and subsonic nozzle (#5). Hence, efforts are made to correlate the associate relation of DOF and WOF (width of focus) against the exit Mach number and diameter. Fig. 4 shows the relevant correlations of the observed DOF/WOF against the outlet Mach number or exit diameter. Generally, DOF increases linearly with the exit Mach number while the WOF is related to exit diameter rather than exit Mach number.

In this study, the outlet pressures and the Mach number of the nozzles are measured. Since the Mach numbers of these nozzles can be either supersonic or sonic, normal shock wave forms before the Pitot tube. The pressure and Mach number we measured from Pitot tube are behind the normal shock, and the relation of the exit Mach number and total pressure before and after the normal shock is given in Eqs. (1) and (2) [10]:

$$M_2^2 = \frac{1 + \frac{\gamma-1}{2} M_1^2}{\gamma M_1^2 - \frac{\gamma-1}{2}} \quad (1)$$

$$\frac{P_{o2}}{P_{o1}} = \frac{1 + \gamma M_1^2 \left(1 + \frac{\gamma-1}{2} M_2^2\right)^{\frac{\gamma}{\gamma-1}}}{1 + \gamma M_2^2 \left(1 + \frac{\gamma-1}{2} M_1^2\right)} \quad (2)$$

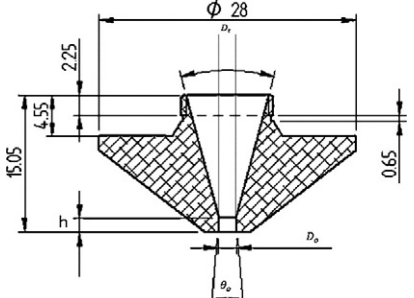
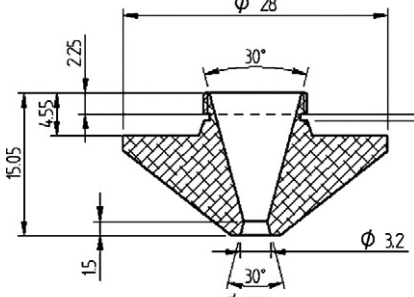
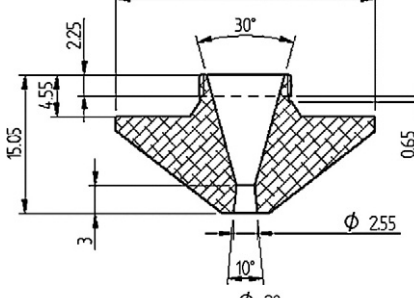
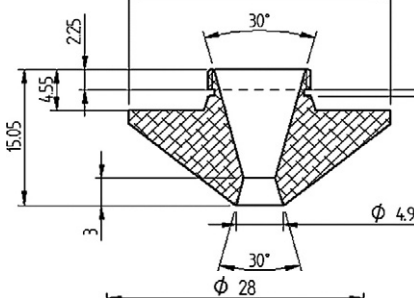
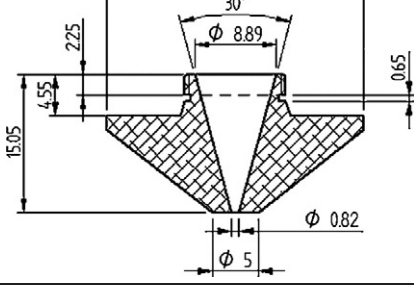
Accordingly the corresponding total pressure, static and dynamic pressures for the test nozzles before and after the normal shock are shown in Fig. 5. The inlet reservoir is kept at 6 bar for all the nozzles. The results show that the total pressure decreases considerably with the outlet Mach number. This is associated with the huge energy loss after the normal shock. The static and dynamic pressure for supersonic nozzles (#1–#4) also shows moderate decline against the exit Mach number as compared to that of total pressure. However, its corresponding dynamic pressure is still higher than that of subsonic nozzle (#5). Despite high Mach number has a better flow shape and longer depth of focus it also causes much larger energy loss.

### 4. Conclusions

This study examines the flow pattern and pressure variation of the nozzles applicable to high power laser cutting and welding. A total of five nozzles having diameter of 0.8–4.0 mm are used for flow visualization and pressure measurement. The depth of focus and the width of focus were measured based on the flow visualization. Based on the foregoing discussions, the following conclusions are made:

1. The depth of focus increases with the rise of exit Mach number while the width of focus increases with the nozzle diameter.

**Table 1**  
Geometrical configuration of the test nozzles.

Nozzle	Configuration	$D_o$ mm	$\theta_o$ degree	$h$	Outlet Mach number
1		2.03	10	1.5	1.76
2		3.2	30	1.5	2.3
3		2.55	10	3	2.02
4		4.96	30	3	3.1
5		0.82	0	0	1

2. The visual results indicate that the supersonic nozzle reveals a more concentrated jet flow even the flow has passed over the depth of focus. On the other hand, appreciate deviation of flow pattern is observed for the subsonic nozzle. This is because the air flow is confined

within the boundary and it reveals a less scattering for supersonic operation.

3. To avoid a larger deviation of flow pattern after DOF for supersonic operation, an exit diameter less than 3.0 mm is recommended.

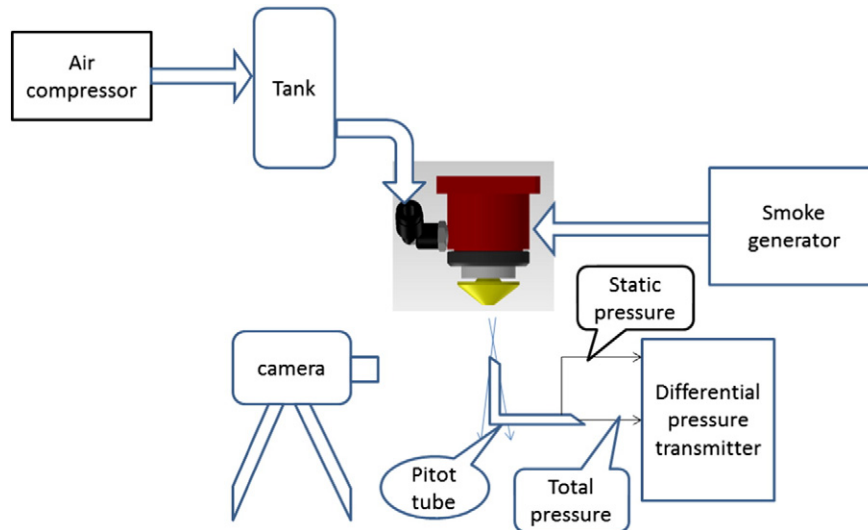


Fig. 1. Schematic of the test facility.

4. The total pressure decreases tremendously with the outlet Mach number due to huge energy loss after the normal shock. The static and dynamic pressure for supersonic nozzles also shows appreciable decline against the exit Mach number. However, its corresponding dynamic pressure is still higher than that of subsonic nozzle.

## References

- [1] H.C. Man, J. Duan, T.M. Vue, Analysis of the dynamic characteristics of gas flow inside a cut kerf under high cut-assist gas pressure, *J. Phys. D: Appl. Phys.* 32 (1999) 1469–1477.
- [2] K. Chen, Y.L. Yao, V. Modi, Gas dynamic effects on laser cut quality, *J. Manuf. Process.* 3 (2001) 38–49.
- [3] K. Chen, Y.L. Yao, V. Modi, Gas jet-workpiece interactions in laser machining, *J. Manuf. Sci. Eng.* 122 (2000) 429–438.
- [4] J. Hu, Z. Zhang, J. Luo, X. Sheng, Simulation and experiment on standoff distance affecting gas flow in laser cutting, *Appl. Math. Model.* 35 (2011) 895–902.
- [5] H.C. Man, J. Duan, T.M. Vue, Modeling the laser fusion cutting process: II. distribution of supersonic gas flow field inside the cut kerf, *J. Phys. D: Appl. Phys.* 34 (2001) 2135–2142.
- [6] H.C. Man, J. Duan, T.M. Vue, Modeling the laser fusion cutting process: III. effects of various process parameters in cut kerf quality, *J. Phys. D: Appl. Phys.* 34 (2001) 2143–2150.
- [7] H.C. Man, J. Duan, T.M. Vue, Design and characteristic analysis of supersonic nozzles for high gas pressure laser cutting, *J. Mater. Process. Technol.* 63 (1997) 217–222.
- [8] S. Guo, H. Jun, L. Lei, Z. Yao, Numerical analysis of supersonic gas-dynamic characteristic in laser cutting, *Opt. Lasers Eng.* 47 (2009) 103–110.
- [9] C.C. Mai, J. Lin, Flow structures around an inclined substrate subjected to a supersonic impinging jet in laser cutting, *Opt. Laser Technol.* 34 (2002) 479–486.
- [10] J.D. Anderson, *Modern Compressible Flow with Historical Perspective*, McGraw-Hill, 2004.

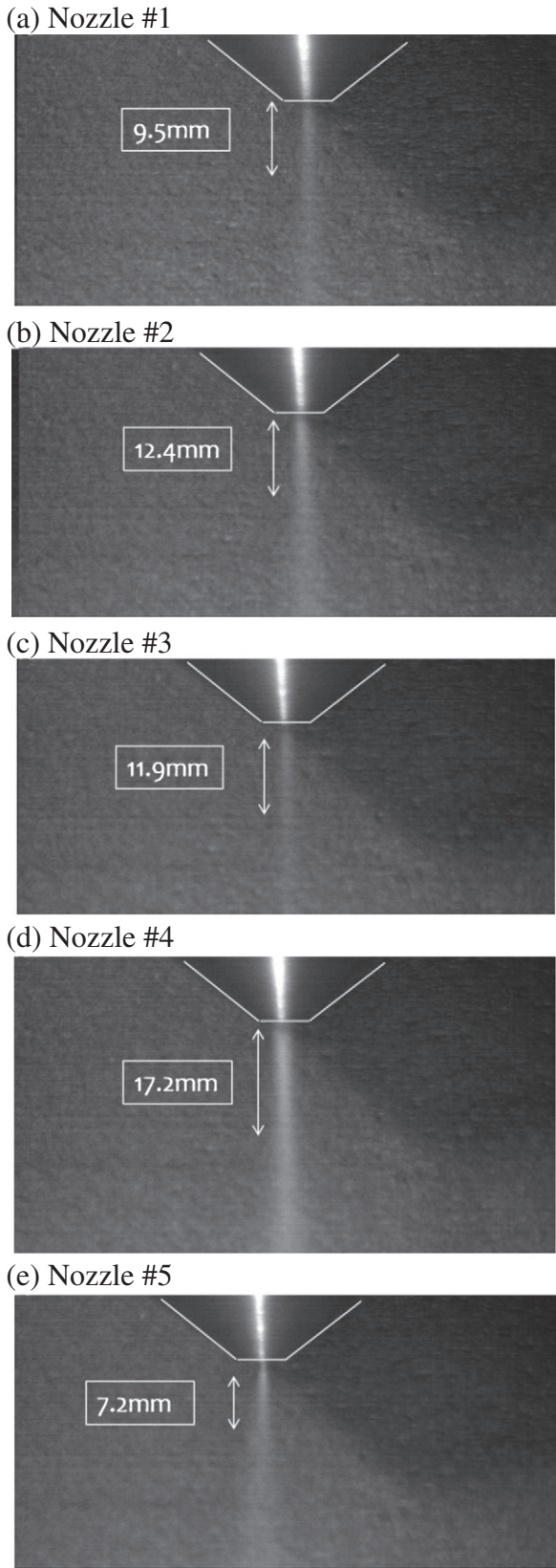


Fig. 2. Visualization of the air flow pattern of the test nozzles.

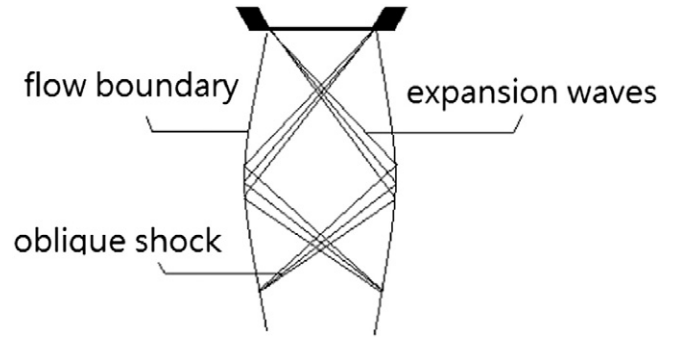
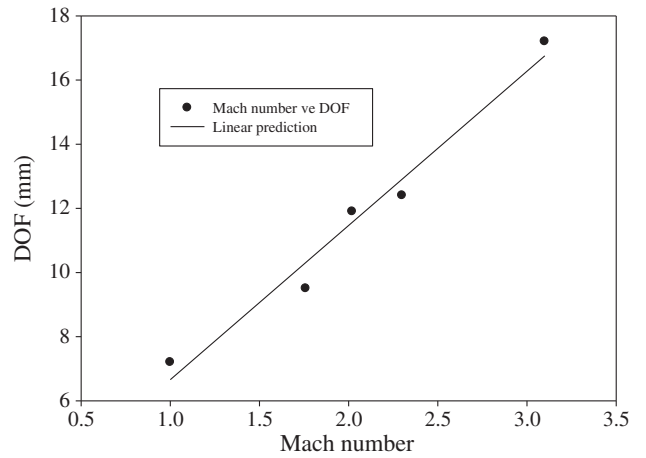


Fig. 3. Flow structure from a supersonic nozzle.

(a) Depth of Focus vs. Mach number



(b) Width of focus vs. nozzle diameter

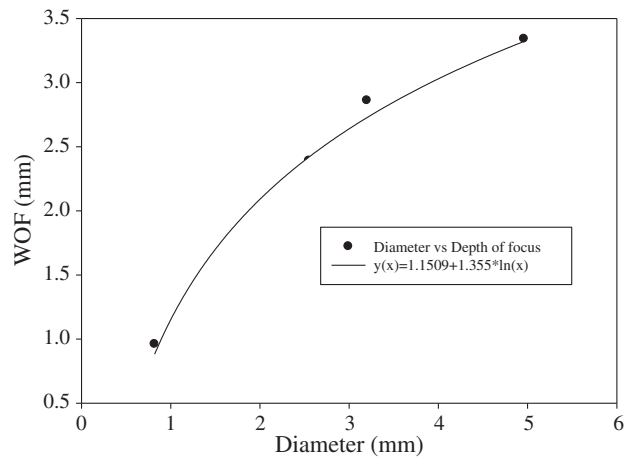
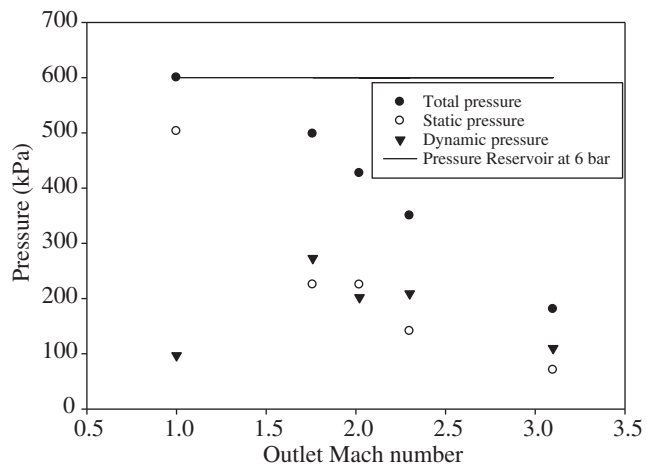


Fig. 4. Depth of focus and width of focus vs. Mach number and nozzle diameter for the test nozzles.



**Fig. 5.** Exit total pressure, static pressure, and dynamic pressure vs. exit Mach number for the test nozzles for an inlet pressure of 6 bar.